

This is the accepted manuscript made available via CHORUS. The article has been published as:

## Isomeric Character of the Lowest Observed $4^{+}$ State in $^{44}\text{S}$

J. J. Parker, IV, I. Wiedenhöver, P. D. Cottle, J. Baker, D. McPherson, M. A. Riley, D. Santiago-Gonzalez, A. Volya, V. M. Bader, T. Baugher, D. Bazin, A. Gade, T. Ginter, H. Iwasaki, C. Loelius, C. Morse, F. Recchia, D. Smalley, S. R. Stroberg, K. Whitmore, D. Weisshaar, A. Lemasson, H. L. Crawford, A. O. Macchiavelli, and K. Wimmer

Phys. Rev. Lett. **118**, 052501 — Published 31 January 2017

DOI: [10.1103/PhysRevLett.118.052501](https://doi.org/10.1103/PhysRevLett.118.052501)

# Isomeric Character of the Lowest Observed $4^+$ State in $^{44}\text{S}$

J.J. Parker IV,<sup>1</sup> I. Wiedenhöver,<sup>1</sup> P.D. Cottle,<sup>1</sup> J. Baker,<sup>1</sup> D. McPherson,<sup>1</sup> M.A. Riley,<sup>1</sup>  
D. Santiago-Gonzalez,<sup>1,\*</sup> A. Volya,<sup>1</sup> V.M. Bader,<sup>2,3</sup> T. Baugher,<sup>2,3</sup> D. Bazin,<sup>2</sup> A. Gade,<sup>2,3</sup>  
T. Ginter,<sup>2</sup> H. Iwasaki,<sup>2,3</sup> C. Loelius,<sup>2,3</sup> C. Morse,<sup>2,3</sup> F. Recchia,<sup>2</sup> D. Smalley,<sup>2</sup> S.R. Stroberg,<sup>2,3,†</sup>  
K. Whitmore,<sup>2,3</sup> D. Weisshaar,<sup>2</sup> A. Lemasson,<sup>4</sup> H.L. Crawford,<sup>5</sup> A.O. Macchiavelli,<sup>5</sup> and K. Wimmer<sup>6,2,‡</sup>

<sup>1</sup>*Department of Physics, Florida State University, Tallahassee, FL, 32306, USA*

<sup>2</sup>*National Superconducting Cyclotron Laboratory, Michigan State University, East Lansing, MI, 48824, USA*

<sup>3</sup>*Department of Physics and Astronomy, Michigan State University, East Lansing, Michigan, 48824, USA*

<sup>4</sup>*Grand Accélérateur National d'Ions Lourds (GANIL), CEA/DSM-CNRS/IN2P3, Caen, France*

<sup>5</sup>*Lawrence Berkeley National Laboratory, Nuclear Science Division,*

*1 Cyclotron Road, Berkeley, CA 94720-8153, USA*

<sup>6</sup>*Department of Physics, Central Michigan University, Mt. Pleasant, Michigan 48859, USA*

(Dated: November 28, 2016)

Previous experiments observed a  $4^+$  state in the  $N=28$  nucleus  $^{44}\text{S}$  and suggested that this state may exhibit a hindered  $E2$ -decay rate, inconsistent with being a member of the collective ground state band. We populate this state via two-proton knockout from a beam of exotic  $^{46}\text{Ar}$  projectiles and measure its lifetime using the recoil distance method with the GRETINA  $\gamma$ -ray spectrometer. The result,  $76(14)_{\text{stat}}(20)_{\text{sys}}$  ps, implies a hindered transition of  $B(E2; 4^+ \rightarrow 2_1^+) = 0.61(19)$  single-particle or Weisskopf units (W.u.) strength and supports the interpretation of the  $4^+$  state as a  $K=4$  isomer, the first example of a high- $K$  isomer in a nucleus of such low mass.

Electromagnetic transition strengths between states in atomic nuclei are valuable indicators of the symmetries in the involved wave functions, especially when quantum-mechanical selection rules lead to hindered  $\gamma$  emission and longer-lived excited states, referred to as isomeric. In a previous work Santiago-Gonzalez *et al.* [1] identified the  $4_1^+$  excited state in the  $N=28$  exotic nucleus  $^{44}\text{S}$  and conjectured – from the overall agreement with shell model predictions – that this state showed properties associated with a high- $K$  isomer. This type of isomerism can occur when the projection of the total angular momentum on the symmetry axis of deformation is a separately conserved quantity, associated with the quantum number  $K$ . The suggestion of a high- $K$  isomer in  $^{44}\text{S}$  was remarkable because this mechanism is known in strongly quadrupole-deformed nuclei of higher mass, where different rotational structures are well separated by  $K$  values and angular-momentum selection rules for  $\gamma$ -ray emission may create long-lived states. A recent review of this phenomenon was given by Walker and Xu in Ref. [2].

The established level structure of  $^{44}\text{S}$  has proven to be a productive laboratory for observing complex phenomena that occur when the nuclear shell structure is modified in neutron-rich isotopes. First, Glasmacher *et al.* [3] measured the  $2_1^+$  state and demonstrated the narrowing of the  $N=28$  major shell closure, which was one of the most cited predictions for near-dripline nuclei at the time. Next, Grévy *et al.* [4] and Force *et al.* [5] identified a low-lying  $0_2^+$  state that demonstrated the coexistence of prolate and spherical structures in  $^{44}\text{S}$  and showed significant mixing between them.

This complex picture of excitations and the surprising suggestion of an isomeric  $4^+$  state by Santiago-Gonzalez *et al.* [1] motivated several theoretical stud-

ies, which separate into two groups. The first group includes beyond-mean field calculations, such as Li *et al.* [6], and Rodríguez and Egido [7] which predict a conventional, deformed level structure with the lowest observed  $4^+$  as part of a rotational band of prolate deformation. The other group are shell-model calculations, such as the one presented in Santiago-Gonzalez *et al.*, which predicts a low-lying, isomeric  $4^+$  state, and the work by Chevrier and Gaudet [8], who affirm the interpretation of Santiago-Gonzalez *et al.* and discuss the coexisting, separate particle-hole configurations in detail. Another shell-model work by Utsuno *et al.* [9] uses the sd<sub>pf</sub>-mu interaction to systematically study the influence of the tensor-force on shape transitions in exotic Si and S isotopes, predicting gamma-soft deformation for  $^{44}\text{S}$ . The two most recent theoretical studies, letter publications by Utsuno and co-workers [10] as well as Egido, Borrajo and Rodríguez [11] will be discussed below, in the context of the experimental result.

All of these theoretical efforts depend centrally on the question to what degree the wave function of the lowest observed  $4^+$  state in  $^{44}\text{S}$  is separated from the other levels, a question that is quantifiable through the lifetime of this state. The current experimental work was performed to measure this lifetime and used nearly identical beam and reaction parameters as the ones described in Ref. [1]. The coupled cyclotron facility at Michigan State University was used to accelerate the primary beam of  $^{48}\text{Ca}$  to 140 MeV/u. The secondary beam of  $^{46}\text{Ar}$  was produced and selected in the A1900 fragment separator, at 99 MeV/u energy and a momentum spread of 1%, with a purity of greater than 90%, and an intensity of  $5.6 \times 10^4$  pps. A two-proton knockout reaction on  $^{46}\text{Ar}$  was used to populate excited states in  $^{44}\text{S}$

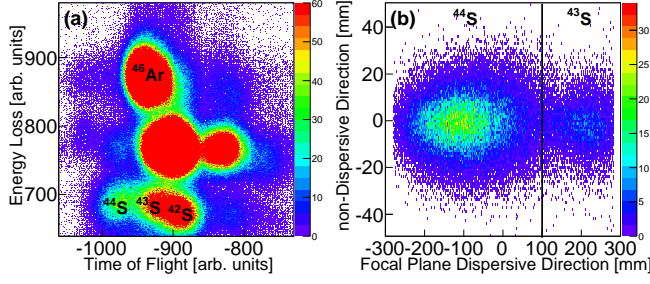


FIG. 1: Spectra associated with the identification of residual nuclei in the S800 spectrograph. Panel a) Residue energy loss versus the path-corrected time-of-flight. Panel b) The focal plane position of Sulfur- reaction residues selected by a gate on the  $^{44}\text{S}$  region in spectrum a). A combination of both conditions allows for a unique separation between events associated with the  $^{44}\text{S}$ ,  $^{43}\text{S}$  and  $^{42}\text{S}$  isotopes.

and the Gamma-Ray Energy Tracking In-beam Nuclear Structure Array (GRETINA) [12] was used to perform high-resolution  $\gamma$ -ray spectroscopy of the fast-moving nuclei. The  $\gamma$  rays were selected in coincidence with the  $^{44}\text{S}$  reaction products in the S800 spectrograph. The event data was analyzed using the GrROOT software package developed by Wimmer *et al.* [13], which implemented the position-resolution capabilities of GRETINA for the reconstruction of cross-scattered  $\gamma$ -rays and Doppler-correction.

At the target location of GRETINA, we used a plunger apparatus [14], which held the 0.5 mm thick  $^9\text{Be}$  target at an adjustable distance from a 1 mm thick Nb degrader and also a thin plastic stripper foil to equilibrate the charge-state distribution of reaction residues. The recoil-distance method allows us to determine the lifetime of excited nuclear states by identifying the  $\gamma$ -rays emitted before and after the recoiling nucleus passes the degrader by detecting their differently Doppler-shifted laboratory-system energies. The velocity of the  $^{44}\text{S}$  residues was found to be 0.42c after the target and 0.36c after the degrader. In the experiment, GRETINA detectors covered laboratory angles ranging from  $22^\circ$  to  $85^\circ$  relative to the beam axis. The  $^{44}\text{S}$  residues were selected using energy loss and time-of-flight measurements from the S800 spectrograph as displayed in Fig.1 correlated with their position in the focal plane. Through these parameters, all three of the observed Sulfur isotopes,  $^{44}\text{S}$ ,  $^{43}\text{S}$  and  $^{42}\text{S}$  could be well separated.

In addition to the recoil-distance measurements, for a period of 14 hours we recorded events from the geometrically identical setup, but with the degrader removed. From this data, we analyzed  $\gamma\gamma$ -coincident events to deduce the placement of  $\gamma$ -transitions in a level scheme. The  $\gamma$ -ray spectrum observed in coincidence with the  $^{44}\text{S}$  reaction residues is displayed in Fig.2, as well as the deduced level scheme. The experimental spectrum is also compared to a Monte-Carlo simulation, which was used

to extract the relative population of excited states in the target-reactions, parameters treated as constant in the subsequent analysis. Details of the Monte-Carlo simulation will be described below.

Our analysis confirms the main transition placements by Santiago-Gonzalez *et al* [1] establishing the  $2_1^+$ ,  $2_3^+$  and  $4_1^+$  excited states. The identification of a level at 3.248 MeV [1], based on the placement of the 1891 keV and 1929 keV pair of transitions could not be confirmed from our  $\gamma\gamma$  coincidence analysis. Consistent with Ref. [1], the 2150 keV transition was tentatively placed populating the ground state, in absence of coincidence information to verify this placement. In addition to the level scheme of Ref. [1] a 1040 keV  $\gamma$  transition was observed to populate the  $2_3^+$  level, confirming the observations of

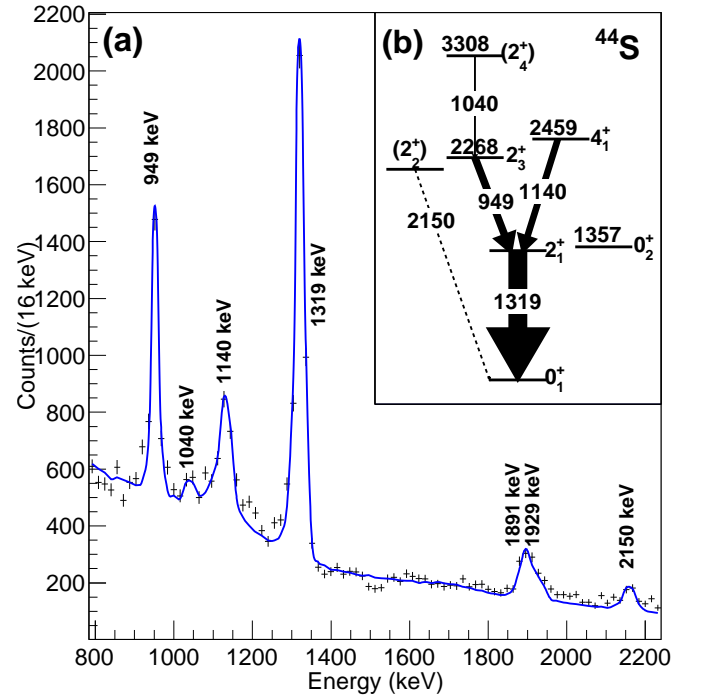


FIG. 2: (Panel a)  $\gamma$ -ray spectrum observed in coincidence with  $^{44}\text{S}$  reaction residues, measured without the energy degrader. The spectrum is compared to a Monte-Carlo simulation of the events (see text). (Panel b) Deduced level scheme for  $^{44}\text{S}$ . The arrow widths are proportional to the observed  $\gamma$ -ray intensities.

The lifetimes of excited states were investigated through the recoil-distance method, where the distance between the  $^9\text{Be}$  target and the Nb degrader was adjusted to 3 mm, 6 mm and 25 mm, which correspond to 24, 48 and 200 ps flight times, respectively, and the events from each distance setting were recorded separately. The experimental spectra are compared to the results of a Monte-Carlo simulation [17], which models the population of excited states, the emission of  $\gamma$ -ray cascades and

the location of  $\gamma$ -ray emission as a function of the level lifetimes. The simulation also includes the energy loss in target- and degrader materials and the emission kinematics in the generation of laboratory-system  $\gamma$  rays. Finally, it simulates the interactions of these  $\gamma$  rays with GRETINA's Germanium crystals and selects the events according to the acceptance of the S800 spectrograph. For comparison with the experimental spectra, the simulated  $\gamma$ -detections are then Doppler corrected in the same way as the measured events.

In our experiment we observe a significant contribution of reactions induced in the degrader, which need to be quantified separately. These reactions are most clearly separated in the spectra recorded for the 25 mm, “long” distance data, which are displayed in Fig.3, gated on the  $^{42}\text{S}$  (panel a) and  $^{44}\text{S}$  (panel b) reaction residues. The events were also selected for laboratory  $\gamma$ -angles below  $45^\circ$  and were Doppler corrected assuming emission from the target position. Because of the long target-degrader distance, all  $\gamma$  rays from reactions in the target are expected to be emitted before the reaction residue nucleus reaches the degrader. Therefore, peaks observed at the correct  $\gamma$ -ray energies stem from reactions in the target, labeled ‘t’ in Fig.3, and peaks at shifted energies stem from reactions induced by the degrader, labeled ‘d’. Those lines are displaced in energy by an over-corrected velocity and an under-corrected  $\gamma$ -detection angle.

The spectra for the 25 mm distance and the Monte-Carlo simulation were used to extract the probability ratio of reactions induced by the target vs. by the degrader, which is 1.30(10) for the population of the  $2_1^+$  state in  $^{42}\text{S}$ . The relative population of the  $2_1^+$ ,  $2_3^+$  and  $4^+$  states in  $^{44}\text{S}$  were determined with values of 1.05(20), 0.85(10) and 1.05(20), respectively. Owing to the fact that  $^{46}\text{Ar}$  beam particles lose energy at a higher rate in material than the Sulfur reaction residues, the locus of the reaction within the target and degrader material also leaves an imprint on the energy of the residues detected in the S800 spectrometer, an effect that was taken into account in the simulation. The 25 mm spectrum of  $^{42}\text{S}$  shows an effect of this correlation, as the S800 acceptance only allowed the highest-momentum residues of  $^{42}\text{S}$  to be detected, enhancing the target-induced peak intensity in the spectrum.

In the following we describe the analysis of the spectra taken at the 3 mm and 6 mm distances with respect to the lifetimes of the  $2_1^+$  state in  $^{42}\text{S}$  and for the  $4^+$  state in  $^{44}\text{S}$ . We are using as fixed parameters the previously determined population yields in target-induced and degrader-induced reactions, normalized by number of counts observed in the 949 keV transition.

The decay transition matrix element of the  $2_1^+$  state in  $^{42}\text{S}$  has been established through Coulomb excitation [18] and is used here as an independent verification of our analysis. In Fig.4 the  $^{42}\text{S}$  data from the 3 mm and 6 mm runs are shown, again selected for laboratory  $\gamma$ -ray angles

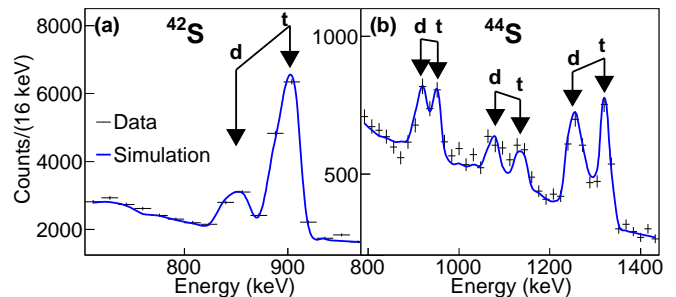


FIG. 3:  $\gamma$ -ray spectra recorded for the target-degrader distance 25 mm, in coincidence with  $^{42}\text{S}$  reaction residues (Panel a) and  $^{44}\text{S}$  (Panel b). For each  $\gamma$ -transition, two peaks are observed, one for target-induced reactions (labeled “t”), and one for degrader-induced reactions (labeled “d”). The simulated spectra were used to determine the ratio of reactions induced by the degrader.

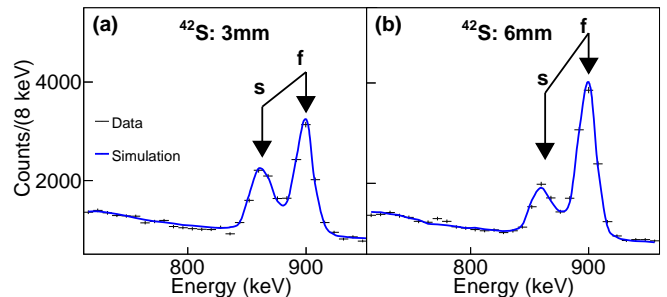


FIG. 4:  $\gamma$ -ray spectra observed in coincidence with  $^{42}\text{S}$ , recorded with the target-degrader distance set to 3 mm (Panel a) and set to 6 mm (Panel b). The relative change in intensities in the fast and slow peaks from 3 mm to 6 mm is an effect of the state’s lifetime. The spectra were fit using a Monte-Carlo simulation (see text).

below  $45^\circ$  and Doppler corrected for emission from the target position. The  $\gamma$ -peaks observed at the correct energies are marked as ‘f’ for “fast” reaction residues, while those shifted to lower energies are marked with an ‘s’ for “slow”. The “slow” peak includes  $\gamma$  rays coming from reactions induced in the target, but emitted after the nucleus slowed down in the degrader, as well as  $\gamma$  rays from degrader-induced reactions. The intensity ratios between the “fast” and “slow” peaks and the change observed between the distances are an effect of the  $2_1^+$  states’ lifetime. The simulated spectrum of the peak region was compared to the experimental spectrum through a  $\chi^2$  analysis, from which a lifetime value of 20.6 ps with a statistical uncertainty of 1.5 ps was extracted, consistent with the Coulomb-excitation value 18.5(33) ps from Ref. [18]. The simulation also included a continuous background of exponential shape in the spectrum, whose parameters were adjusted globally for the target-degrader runs. The uncertainty in the adopted background parameters did not influence the extracted lifetime values significantly in comparison to the statistical errors.

The lifetime of the  $4^+$  state in  $^{44}\text{S}$  was determined in an analogous way. The spectra for the 3 mm and 6 mm runs are shown in Fig. 5. Here, we also select the upper half of the residue momenta detected in the S800 spectrograph, creating an enhancement of the target-induced events and the RDM-effects in the data. The 1140 keV and the 1319 keV  $\gamma$  transitions both exhibit two distinct components, whereas the 949 keV transition only shows one peak with a shape indicative of a very fast decay. From this analysis an upper limit of 3 ps was adopted for the lifetime of the 2268 keV state.

The 1140 keV line, identified with the  $4^+ \rightarrow 2_1^+$  transition, exhibits a lifetime effect similar to the one observed for the  $^{42}\text{S}$  peak discussed above, only with a larger fraction in the “slow” components, indicative of a longer lifetime. Fig. 5 compares the spectrum to the simulation with the adopted 76 ps lifetime and – to illustrate the magnitude of the lifetime effects – a simulation for a short, 3.5 ps lifetime. It should be noted that the delayed character of the 1140 keV transition also leads to a delayed emission of the 1319 keV  $2_1^+ \rightarrow 0_1^+$  transition in cascade.

We performed a  $\chi^2$  analysis testing the 3 mm and 6 mm spectra against the respective Monte-Carlo simulations over a range of hypothetical lifetimes, which provided a value of  $76(14)_{\text{stat}}(20)_{\text{sys}}$  ps at a reduced  $\chi^2 = 2.7$ . The systematic uncertainty is estimated by allowing a different relative yield for the 1140 keV transition in the degrader-induced reactions.

The deduced lifetime for the  $4^+$  state corresponds to a reduced matrix element for the 1140 keV transition of  $B(E2; 4^+ \rightarrow 2_1^+) = 5.6(18) e^2 fm^4$  or  $0.61(19)$  W.u. . For comparison, the ground state transition matrix element  $B(E2; 2_1^+ \rightarrow 0_1^+) = 63(18) e^2 fm^4$  [3] corresponds to  $7(2)$  single-particle or “Weisskopf” units (W.u.), which is indicative of moderate collectivity.

In almost all even-even nuclei the  $4_1^+$  state is a

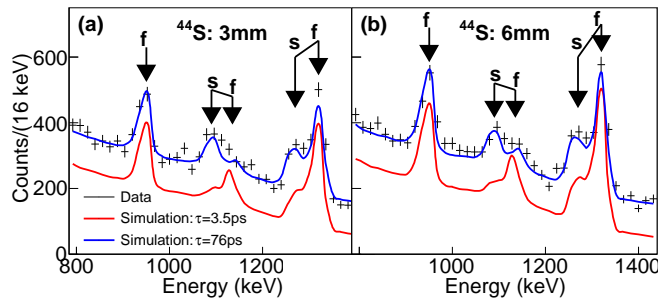


FIG. 5:  $\gamma$ -ray spectra observed in coincidence with  $^{44}\text{S}$ , recorded with the target–degrader distance set to 3mm (Panel a) and set to 6mm (Panel b). The spectra are compared to a Monte-Carlo simulation for the adopted lifetime of the  $4^+$  state (76 ps) and, for comparison and horizontally offset, a short lifetime of 3.5 ps. The 949 keV peak shows characteristics of a prompt emission.

quadrupole excitation built on the lowest  $2_1^+$ . For  $^{44}\text{S}$  all theoretical studies predict such a collective rotational  $4^+$  state to exist and to decay with a much larger  $B(E2; 4_{\text{rot}}^+ \rightarrow 2_1^+)$  transition matrix element of values varying between 9.1 W.u. [10] and 13.5 W.u. [11]. The deduced value of  $0.61(19)$  W.u. for the decay of the observed  $4^+$  state is evidence that this state is not a member of the ground-state rotational band, confirming the hypothesis put forth by Santiago-Gonzalez *et al.* [1]. The hindered  $B(E2)$  value also means that the  $4^+$  at 2459 keV shows very little mixing with the rotational  $4^+$  state – which is so far unobserved, but must exist – and which is predicted by theoretical studies to lie within 250 keV of the observed  $4^+$ .

The two most recent theoretical publications, Utsumo and co-workers [10] as well as Egido, Borrajo and Rodríguez [11] placed an emphasis on the properties of the mean field and the symmetries of the intrinsic frame wave function required to produce such a low-lying isomeric  $4^+$  state. Utsumo and co-workers analyzed the shell-model wave functions in the intrinsic frame of reference by means of a Variation After Angular Momentum Projection (AM-VAP) method and found that the  $4_1^+$  state is dominated by an almost pure (93%)  $K=4$  configuration, while showing a maximally triaxial shape with  $\gamma = 28^\circ$  [10] and moderate quadrupole deformation  $\beta_2 = 0.23$ . In their subsequent publication [11] Egido, Borrajo and Rodríguez expanded the parameter space of their symmetry conserving configuration mixing (SCCM) calculation and described an isomeric  $4^+$  state in  $^{44}\text{S}$  with very similar properties, a predominant  $K=4$  configuration, strong triaxiality and large deformation  $\beta_2 \approx 0.28 - 0.36$ . Both studies predict a very small decay matrix element of  $0.1 e^2 fm^4$  [10] and  $1.4 e^2 fm^4$  [11], values that are smaller than the observed  $5.6(18) e^2 fm^4$ , but in agreement with the isomeric character of the  $4^+$  state.

The purity of the  $4^+$  wave function in the context of near-maximum triaxiality is a property that remains surprising, as noted by both above-mentioned publications. Both studies also noted that the intrinsic-frame wave function of the isomeric  $4^+$  state violates time-reversal symmetry, stated to be nearly maximal in Ref. [10]. It is tempting to speculate whether this property, not present in conventional collective excitations with pure  $K$ -quantum numbers, points to a separate implicit symmetry of the mean field leading to an orthogonalization of isomeric and rotational  $4^+$  states.

Given the exotic structure of the isomeric  $4^+$  state, the search for the collective rotational  $4^+$  state gains additional significance. In this context it is interesting to note that Santiago-Gonzalez *et al.* [1], who were using the same reaction as the present work, were able to reproduce the population of the isomeric  $4^+$  at a cross section of  $0.019(4)$  mb, through a calculation based on an Eikonal approximation and shell-model wave func-

tions. The same calculation also produced a cross section smaller than  $1 \mu\text{b}$  towards the collective  $4^+$  state, explained by a lack of overlap with the  $^{46}\text{Ar}$  ground state and being consistent with its non-observation. In pursuit of the collective  $4^+$  state, additional spectroscopic studies with other excitation mechanisms and modern high-resolution  $\gamma$ -spectroscopy methods are called for.

In summary, we have measured the average lifetime of the 2459 keV  $4^+$  state in  $^{44}\text{S}$  to be  $76(14)_{\text{stat}}(20)_{\text{sys}}$  ps, which corresponds to a reduced transition matrix element of only  $B(E2; 4^+ \rightarrow 2_1^+) = 0.61(19)$  W.u. This value demonstrates that the observed  $4^+$  state is not a member of the ground state rotational band and that it is remarkably pure, despite the likelihood that the rotational  $4^+$  state is located within a few hundred keV excitation energy of the observed  $4^+$ . The properties of the observed  $4^+$  state establish a new kind of isomerism in light exotic nuclei, to which theoretical calculations assign a near-pure  $K=4$  character at the same time as moderate or strong, triaxial quadrupole deformation. The presence of such configurations in the breaking of the  $N=28$  shell closure provides new experimental and theoretical opportunities in the study of the shell structure in exotic nuclei.

This work is supported in part by the National Science Foundation (NSF) under Grant Nos. PHY-1064819 and PHY-1401574, by the Department of Energy (DOE) National Nuclear Security Administration under award number DE-NA0000979. GRETINA was funded by the US DOE Office of Science. Operation of the array at NSCL was supported by the NSF under Cooperative Agreement PHY-1102511 and by the DOE under Contract No. DE-AC02-05CH11231.

---

\* Current address: Department of Physics and Astronomy, Louisiana State University, Baton Rouge, LA 70803, USA

† Current address: TRIUMF, 4004 Wesbrook Mall, Vancouver, British Columbia, Canada V6T 2A3

‡ Current address: The University of Tokyo, Hongo, Bunkyo-ku, Tokyo 113-0033, Japan

- [1] D. Santiago-Gonzalez, I. Wiedenhöver, V. Abramkina, M. L. Avila, T. Baugher, D. Bazin, B. A. Brown, P. D. Cottle, A. Gade, T. Glasmacher, et al., *Phys.Rev. C* **83**, R061305 (2011).
- [2] P. M. Walker and F. R. Xu, *Physica Scripta* **91**, 013010 (2016), URL <http://stacks.iop.org/1402-4896/91/i=1/a=013010>.
- [3] T. Glasmacher, B. A. Brown, M. J. Chromik, P. D. Cot-

- tle, M. Fauerbach, R. W. Ibbotson, K. W. Kemper, D. J. Morrissey, H. Scheit, D. W. Sklenicka, et al., *Phys.Lett.* **395B**, 163 (1997).
- [4] S. Grévy, F. Negoita, I. Stefan, N. L. Achouri, J. C. Angelique, B. Bastin, R. Borcea, A. Buta, J. M. Daugas, F. De Oliveira, et al., *Eur.Phys.J. A* **25**, Supplement 1, 111 (2005).
- [5] C. Force, S. Grévy, L. Gaudefroy, O. Sorlin, L. Caceres, F. Rotaru, J. Mrazek, N. L. Achouri, J. C. Angelique, F. Azaiez, et al., *Phys.Rev.Lett.* **105**, 102501 (2010).
- [6] Z. P. Li, J. M. Yao, D. Vretenar, T. Niksic, H. Chen, and J. Meng, *Phys.Rev. C* **84**, 054304 (2011).
- [7] T. R. Rodriguez and J. L. Egido, *Phys.Rev. C* **84**, 051307 (2011).
- [8] R. Chevrier and L. Gaudefroy, *Phys.Rev. C* **89**, 051301 (2014).
- [9] Y. Utsuno, T. Otsuka, B. A. Brown, M. Honma, T. Mizusaki, and N. Shimizu, *Phys.Rev. C* **86**, 051301(R) (2012).
- [10] Y. Utsuno, N. Shimizu, T. Otsuka, T. Yoshida, and Y. Tsunoda, *Phys.Rev.Lett.* **114**, 032501 (2015).
- [11] J. L. Egido, M. Borrajo, and T. R. Rodríguez, *Phys. Rev. Lett.* **116**, 052502 (2016), URL <http://link.aps.org/doi/10.1103/PhysRevLett.116.052502>.
- [12] S. Paschalis, I. Lee, A. Macchiavelli, C. Campbell, M. Cromaz, S. Gros, J. Pavan, J. Qian, R. Clark, H. Crawford, et al., *Nuclear Instruments and Methods in Physics Research Section A: Accelerators, Spectrometers, Detectors and Associated Equipment* **709**, 44 (2013), ISSN 0168-9002, URL <http://www.sciencedirect.com/science/article/pii/S0168900213000508>.
- [13] K. Wimmer and E. Lunderberg, GRoot software package, to be published, URL <http://nucl.phys.s.u-tokyo.ac.jp/wimmer/software.php>.
- [14] H. Iwasaki, A. Dewald, T. Braunroth, C. Fransen, D. Smalley, A. Lemasson, C. Morse, K. Whitmore, and C. Loelius, *Nuclear Instruments and Methods in Physics Research Section A: Accelerators, Spectrometers, Detectors and Associated Equipment* **806**, 123 (2016), ISSN 0168-9002, URL <http://www.sciencedirect.com/science/article/pii/S0168900215011626>.
- [15] L. A. Riley, P. Adrich, N. Ahsan, T. R. Baugher, D. Bazin, B. A. Brown, J. M. Cook, P. D. Cottle, C. A. Diget, A. Gade, et al., *Phys.Rev. C* **86**, 047301 (2012).
- [16] L. Caceres, D. Sohler, S. Grévy, O. Sorlin, Z. Dombradi, B. Bastin, N. L. Achouri, J. C. Angelique, F. Azaiez, D. Baiborodin, et al., *Phys.Rev. C* **85**, 024311 (2012).
- [17] P. Adrich, D. Enderich, D. Miller, V. Moeller, R. Norris, K. Starosta, C. Vaman, P. Voss, and A. Dewald, *Nuclear Instruments and Methods in Physics Research Section A: Accelerators, Spectrometers, Detectors and Associated Equipment* **598**, 454 (2009).
- [18] H. Scheit, T. Glasmacher, B. A. Brown, J. A. Brown, P. D. Cottle, P. G. Hansen, R. Harkewicz, M. Hellstrom, R. W. Ibbotson, J. K. Jewell, et al., *Phys.Rev.Lett.* **77**, 3967 (1996).